12th International Conference on Applications of Statistics and Probability in Civil Engineering, ICASP12
Vancouver, Canada, July 12-15, 2015

Efficient Optimal Design-Under-Uncertainty of Passive Structural Control Devices

Subhayan De
Graduate Research Assistant, Sonny Astani Department of Civil and Environmental Engineering, University of Southern California, Los Angeles, California, USA

Steven F. Wojtkiewicz
Associate Professor, Department of Civil and Environmental Engineering, Clarkson University, Potsdam, New York, USA

Erik A. Johnson
Professor, Sonny Astani Department of Civil and Environmental Engineering, University of Southern California, Los Angeles, California, USA

ABSTRACT: This paper proposes a computationally efficient framework for design optimization under uncertainty for structures with local nonlinearities. To reduce the high computational cost of Monte Carlo simulation of such problems, an exact model reduction to a low-order Volterra integral equation is used to accelerate each simulation, and variance-reduced sampling is used to reduce the number of simulations required for the uncertainty quantification. This optimization framework is applied to a benchmark cable-stayed bridge problem, designing one pair of passive tuned mass dampers given a pair of uncertain passive power law dampers, providing significant gains in computational efficiency, two orders of magnitude, compared to traditional approaches.

1. INTRODUCTION

Robust design in presence of uncertainties in material, loading or topological characteristics of a structure has been investigated using convex optimization, neural network and evolutionary algorithms (Enevoldsen and Sørensen, 1994; Sandgren and Cameron, 2002; Papadrakakis and Lagaros, 2002; Zang et al., 2005; Calafiore and Dabbene, 2008). Over the past few decades, reliability-based design optimization of these uncertain structures has been investigated using single and multi-objective optimization both approaches (Frangopol, 1985; Gasser and Schuëller, 1997; Tu et al., 1999; Adeli, 2002; Beck et al., 1996, 1999).

While many design-level earthquakes generate superstructure responses that are elastic and linear, passive structural control devices embedded in the structure often have nonlinear characteristics (e.g., power-law, bilinear and/or hysteretic behavior), introducing local nonlinearities into an otherwise linear model and, therefore, requiring either simplifying approximations or a full nonlinear simulation to evaluate response characteristics. If some parts of such a model are also uncertain (e.g., characteristics of the same, or other, structural control elements or other localized components), then Monte Carlo sampling can be used for uncertainty characterization; this, in turn, further increases the computational requirements for analysis of such systems. The optimal design of passive nonlinear control devices requires repeated solutions of the nonlinear system. Multiplying these three costs — nonlinear simulation, Monte Carlo sampling, and design parameter iterations — often creates a significant computational burden, so there is a clear advantage in the design-under-uncertainty problem for a computationally efficient approach to solve for the response of locally nonlinear systems.

A conventional nonlinear solver (e.g., `ode45` in MATLAB) cannot exploit the localized nature of the

nonlinearities. However, a method recently proposed by the last two authors (Gaurav et al., 2011) develops an exact nonlinear model reduction for systems of this type, resulting in a low-order nonlinear Volterra integral equation, providing a significant computational speedup compared to `ode45`. Further, the authors recently proposed (Kamalzare et al., 2015) capitalizing on the local nature of design variables to make design optimization simulations more computationally efficient.

This paper extends the scope of that work by additionally incorporating localized uncertainties into the model to arrive at a computationally-efficient design-under-uncertainty framework for systems that are mostly linear and deterministic but that have localized nonlinear and uncertain elements. The proposed framework is illustrated using a finite element model of the Bill Emerson Memorial Bridge in Cape Girardeau, Missouri, consisting of 579 nodes, 162 beam elements, 128 cable elements, 420 rigid links and 134 nodal masses, resulting in a 419 degree-of-freedom (DOF) model after removing dependent or boundary DOFs (Dyke et al., 2003). The optimal design of parameters of linear and nonlinear structural control devices is performed using the proposed approach while key elements of the structure are uncertain (e.g., a previously installed passive damping device). The proposed method is shown to provide significant reduction in required computation times, relative to ode45, while delivering the same level of accuracy.

2. METHODOLOGY

2.1. Efficient response with local uncertainties

Following Gaurav et al. (2011), let the nonlinear structure model be given in state space by

$$\begin{aligned}\dot{\mathbf{X}}(t) &= \mathbf{A}\mathbf{X}(t)+\mathbf{B}\mathbf{w}(t)+\mathbf{L}_{\mathrm{u}}\mathbf{g}_{\mathrm{u}}(\overline{\mathbf{X}}_{\mathrm{u}}(t);\boldsymbol{\delta}) \\ &\qquad +\mathbf{L}_{\mathrm{d}}\mathbf{g}_{\mathrm{d}}(\overline{\mathbf{X}}_{\mathrm{d}}(t);\boldsymbol{\theta}) \\ &= \mathbf{A}\mathbf{X}(t)+\mathbf{B}\mathbf{w}(t)+\mathbf{L}\mathbf{g}(\overline{\mathbf{X}}(t);\boldsymbol{\delta},\boldsymbol{\theta}) \\ \mathbf{Y}(t) &= \mathbf{C}\mathbf{X}(t)+\mathbf{D}\mathbf{w}(t)+\mathbf{E}_{\mathrm{u}}\mathbf{g}_{\mathrm{u}}(\overline{\mathbf{X}}_{\mathrm{u}}(t);\boldsymbol{\delta}) \\ &\qquad +\mathbf{E}_{\mathrm{d}}\mathbf{g}_{\mathrm{d}}(\overline{\mathbf{X}}_{\mathrm{d}}(t);\boldsymbol{\theta}) \\ &= \mathbf{C}\mathbf{X}(t)+\mathbf{D}\mathbf{w}(t)+\mathbf{E}\mathbf{g}(\overline{\mathbf{X}}(t);\boldsymbol{\delta},\boldsymbol{\theta}) \\ \mathbf{X}(0) &= \mathbf{x}_0\end{aligned} \tag{1}$$

where $\mathbf{X}(t)$ is the $n\times 1$ state vector; $\mathbf{A}$ is the $n\times n$ state matrix, $\mathbf{w}$ is an $m\times 1$ external excitation; $\mathbf{B}$ is the $n\times m$ influence matrix; $\mathbf{g}_{\mathrm{u}}(\cdot;\cdot)$ is an $n_{\mathrm{g,u}}\times 1$ function of a subset $\overline{\mathbf{X}}_{\mathrm{u}}(t)=\mathbf{G}_{\mathrm{u}}\mathbf{X}(t)$ of states and uncertain parameters $\boldsymbol{\delta}$; $\mathbf{g}_{\mathrm{d}}(\cdot;\cdot)$ is an $n_{\mathrm{g,d}}\times 1$ function of a subset $\overline{\mathbf{X}}_{\mathrm{d}}(t)=\mathbf{G}_{\mathrm{d}}\mathbf{X}(t)$ of states and design parameters $\boldsymbol{\theta}$; $\mathbf{L}_{\mathrm{u}}$ is an $n\times n_{\mathrm{g,u}}$ influence matrix mapping to all states from the force vector $\mathbf{g}_{\mathrm{u}}$ arising due to uncertain parameters; $\mathbf{L}_{\mathrm{d}}$ is an $n\times n_{\mathrm{g,d}}$ influence matrix mapping to all states from the force vector $\mathbf{g}_{\mathrm{d}}(\cdot;\cdot)$ arising due to design parameters; $\mathbf{D}$ is an $n_{\mathrm{y}}\times m$ influence matrix; $\mathbf{E}_{\mathrm{u}}$ and $\mathbf{E}_{\mathrm{d}}$ are $n_{\mathrm{y}}\times n_{\mathrm{g,u}}$ and $n_{\mathrm{y}}\times n_{\mathrm{g,d}}$ influence matrices, respectively; and $\mathbf{x}_0$ is the initial condition. State subsets $\overline{\mathbf{X}}_{\mathrm{u}}(t)$ and $\overline{\mathbf{X}}_{\mathrm{d}}(t)$ are $n_{\mathrm{o,u}}\times 1$ and $n_{\mathrm{o,d}}\times 1$ vectors, respectively, with $n_{\mathrm{o,u}}, n_{\mathrm{o,d}} \ll n$. Output $\mathbf{Y}(t)$ is an $n_{\mathrm{y}}\times 1$ vector. Combining the forces from the uncertainties and nonlinearities, $\mathbf{L}=[\mathbf{L}_{\mathrm{u}}^{\mathrm{T}} \quad \mathbf{L}_{\mathrm{d}}^{\mathrm{T}}]^{\mathrm{T}}$ is $n\times n_{\mathrm{o}}$ and $\mathbf{g}(\overline{\mathbf{X}}(t);\boldsymbol{\delta},\boldsymbol{\theta}) = [\mathbf{g}_{\mathrm{u}}^{\mathrm{T}}(\overline{\mathbf{X}}_{\mathrm{u}}(t);\boldsymbol{\delta}) \quad \mathbf{g}_{\mathrm{d}}^{\mathrm{T}}(\overline{\mathbf{X}}_{\mathrm{d}}(t);\boldsymbol{\theta})]^{\mathrm{T}}$ is $n_{\mathrm{o}}\times 1$, where $n_{\mathrm{o}}\le(n_{\mathrm{g,u}}+n_{\mathrm{g,d}})$. Similarly, $\overline{\mathbf{X}}(t) = [\overline{\mathbf{X}}_{\mathrm{u}}^{\mathrm{T}}(t) \quad \overline{\mathbf{X}}_{\mathrm{d}}^{\mathrm{T}}(t)]^{\mathrm{T}}=\mathbf{G}\mathbf{X}(t)$ for $\mathbf{G}=[\mathbf{G}_{\mathrm{u}}^{\mathrm{T}} \quad \mathbf{G}_{\mathrm{d}}^{\mathrm{T}}]^{\mathrm{T}}$.

The nominal linear system corresponding to the nonlinear system in (1) is

$$\dot{\mathbf{x}}(t)=\mathbf{A}\mathbf{x}(t)+\mathbf{B}\mathbf{w}(t), \qquad \mathbf{x}(0)=\mathbf{x}_0 \tag{2}$$

Using the principle of superposition, the response of the system can be divided into two parts: the solution $\mathbf{x}(t)$ of the nominal linear system in (2) and the contribution of the functions $\mathbf{g}(\overline{\mathbf{X}})$ which can be written

$$\begin{aligned}\mathbf{x}(t) &= e^{\mathbf{A}t}\mathbf{x}_0+\int_0^t \mathbf{H}_{\mathrm{B}}(t-s)\mathbf{w}(s)\mathrm{d}s, \\ \mathbf{x}^{(\mathrm{nl})}(t) &= \int_0^t \mathbf{H}_{\mathrm{L}}(t-s)\mathbf{g}(\overline{\mathbf{X}}(s);\boldsymbol{\delta},\boldsymbol{\theta})\mathrm{d}s\end{aligned} \tag{3}$$

where the impulse responses are given by $\mathbf{H}_{\mathrm{B}}(t)=e^{\mathbf{A}t}\mathbf{B}$ and $\mathbf{H}_{\mathrm{L}}(t)=e^{\mathbf{A}t}\mathbf{L}$. The total response is the superposition of these two responses; *i.e.*, $\mathbf{X}=\mathbf{x}+\mathbf{x}^{(\mathrm{nl})}$. For any value of $\boldsymbol{\delta}$ and $\boldsymbol{\theta}$, the solution of (3) can be computed efficiently with the following:

$$\begin{aligned}\mathbf{p}(t) &= \mathbf{g}(\overline{\mathbf{X}}(t);\boldsymbol{\delta},\boldsymbol{\theta}); \\ \overline{\mathbf{X}}(t) &= \overline{\mathbf{x}}(t)+\int_0^t \overline{\mathbf{H}}_{\mathrm{L}}(t-s)\mathbf{p}(s)\mathrm{d}s\end{aligned} \tag{4}$$

where $\overline{\mathbf{x}}(t)=\mathbf{G}\mathbf{x}(t)$ and $\overline{\mathbf{H}}_{\mathrm{L}}(t)=\mathbf{G}\mathbf{H}_{\mathrm{L}}(t)$. The set of equations (4) can be combined into:

$$\mathbf{p}(t)-\mathbf{g}\left(\overline{\mathbf{x}}+\int_0^t \overline{\mathbf{H}}_{\mathrm{L}}(t-s)\mathbf{p}(s)\mathrm{d}s;\boldsymbol{\delta},\boldsymbol{\theta}\right)=0 \tag{5}$$

Equation (5) is a nonlinear vector Volterra integral equation (NVIE) written in nonstandard form, which can be solved by a Newton-Gregory integration scheme (Linz, 1985). In the algorithm proposed in the authors' earlier works, the Newton-Gregory integration is coupled with a recursive FFT formulation to drastically reduce the cost of computation of the required convolution.

Of course, any redundant columns in $\mathbf{L}$ (*e.g.*, if two devices are collocated) can be eliminated and the dimension of $\mathbf{g}(\overline{\mathbf{X}}(t);\boldsymbol{\delta},\boldsymbol{\theta})$ can be reduced, simplifying the solution of NVIE (5). Further, any redundant columns of $\mathbf{G}$ can be eliminated and the dimensions of $\overline{\mathbf{x}}$ and $\overline{\mathbf{X}}$ can be reduced.

2.2. Design optimization under uncertainty

Two design-under-uncertainty objectives are employed herein: worst-case design and average design (Calafiore and Dabbene, 2008). A brief description of these two procedures follows.

2.2.1. Worst case design

In this design method, the structure or control device is designed for the case when the cost function is maximized over the domain of uncertainty with constraints satisfied, known as worst-case design. This design optimization problem can be defined as

$$\begin{aligned} &\min_{\boldsymbol{\theta}\in\boldsymbol{\Theta}} \max_{\boldsymbol{\delta}\in\boldsymbol{\Delta}} J(\mathbf{Y}(t);\boldsymbol{\theta},\boldsymbol{\delta}) \\ &\text{subject to} \quad \mathbf{h}(\mathbf{Y}(t);\boldsymbol{\theta},\boldsymbol{\delta}_{\max}(\boldsymbol{\theta})) \le \mathbf{0} \quad \text{a.s.}^{1} \end{aligned} \tag{6}$$

where $J(\cdot)$ and $\mathbf{h}(\cdot)$ may be functionals of the entire trajectory of $\mathbf{Y}$; the set of all possible values of design parameter $\boldsymbol{\theta}$ is denoted by $\boldsymbol{\Theta}$; $\boldsymbol{\Delta}$ represents a probability space $\{\Omega,\mathbb{P},\mathcal{F}\}$ with sample space Ω, probability measure $\mathbb{P}$, and σ-algebra $\mathcal{F}$ corresponding to the uncertainty defined for the problem; $\boldsymbol{\delta}_{\max}(\boldsymbol{\theta}) \in \boldsymbol{\Delta}$ is the uncertainty realization which, for a particular design $\boldsymbol{\theta}$, maximizes $J(\mathbf{Y}(t);\boldsymbol{\theta},\boldsymbol{\delta})$ subject to the constraint $\mathbf{h}$; and $J(\cdot)$ is assumed concave in $\boldsymbol{\delta}$. The analytical solution of (6) may not always be possible. However, with samples $\{\boldsymbol{\delta}_i\}_{i=1}^{N_{\boldsymbol{\delta}}}$ from $\boldsymbol{\Delta}$, one may approximate the problem as

$$\begin{aligned} &\min_{\boldsymbol{\theta}\in\boldsymbol{\Theta}} \max_{i=1,\ldots,N_{\boldsymbol{\delta}}} J(\mathbf{Y}(t);\boldsymbol{\theta},\boldsymbol{\delta}_i) \\ &\text{subject to} \quad \mathbf{h}(\mathbf{Y}(t);\boldsymbol{\theta},\boldsymbol{\delta}_{i,\max}(\boldsymbol{\theta})) \le \mathbf{0} \end{aligned} \tag{7}$$

[1] Almost sure (a.s.) event happens with probability 1.

where $\boldsymbol{\delta}_{i,\max}(\boldsymbol{\theta})$ corresponds to the sample which, for a particular design $\boldsymbol{\theta}$, maximizes $J(\mathbf{Y}(t);\boldsymbol{\theta},\boldsymbol{\delta})$ subject to the constraint $\mathbf{h}$.

2.2.2. Average design

In the second method of design considered, the expected value of cost is minimized while keeping the constraints satisfied. This optimization problem is defined as

$$\begin{aligned} &\min_{\boldsymbol{\theta}\in\boldsymbol{\Theta}} \mathbb{E}_{\delta}[J(\mathbf{Y}(t);\boldsymbol{\theta},\boldsymbol{\delta})] \\ &\text{subject to} \quad \mathbf{h}(\mathbf{Y}(t);\boldsymbol{\theta},\boldsymbol{\delta}) \le \mathbf{0} \quad \text{a.s.} \end{aligned} \tag{8}$$

With samples $\{\boldsymbol{\delta}_i\}_{i=1}^{N_{\boldsymbol{\delta}}}$ from $\boldsymbol{\Delta}$,

$$\begin{aligned} &\min_{\boldsymbol{\theta}\in\boldsymbol{\Theta}} \frac{1}{N_{\delta}} \sum_{i=1}^{N_{\boldsymbol{\delta}}} J(\mathbf{Y}(t);\boldsymbol{\theta},\boldsymbol{\delta}_i) \\ &\text{subject to} \quad \mathbf{h}(\mathbf{Y}(t);\boldsymbol{\theta},\boldsymbol{\delta}_i) \le \mathbf{0} \end{aligned} \tag{9}$$

3. NUMERICAL EXAMPLE

3.1. Cable-stayed bridge model

The example used to demonstrate the framework is a numerical model of the Bill Emerson Memorial Bridge, a cable stayed bridge, built in 2003 across the Mississippi river between Cape Girardeau, Missouri, and East Cape Girardeau, Illinois. A finite element model of the bridge superstructure, developed in Dyke et al. (2003) and shown in Fig. 1, consists of 579 nodes, 128 cable elements, 162 beam elements, 420 rigid links and 134 nodal masses. (The version of the model used herein has no connection between deck and tower except through the cables so as to allow energy dissipator devices placed between the deck and a tower.) The initial 3474 degree-of-freedom (DOF) model, which describes the superstructure's linear motion about the static equilibrium, is reduced to 909 DOFs when the boundary conditions are imposed and the slave DOFs removed. Static condensation is then applied to eliminate DOFs with small contribution to the global response, resulting in the final 419 DOF model, which is available publicly (Dyke et al., 2003) and which is used here. The equation of motion of this final bridge model is given by

$$\mathbf{M}_{\mathrm{s}}\ddot{\mathbf{u}}_{\mathrm{s}}(t) + \mathbf{C}_{\mathrm{s}}\dot{\mathbf{u}}_{\mathrm{s}}(t) + \mathbf{K}_{\mathrm{s}}\mathbf{u}_{\mathrm{s}}(t) = -\mathbf{M}_{\mathrm{s}}\mathbf{r}\ddot{u}_{\mathrm{g}}(t) \tag{10}$$

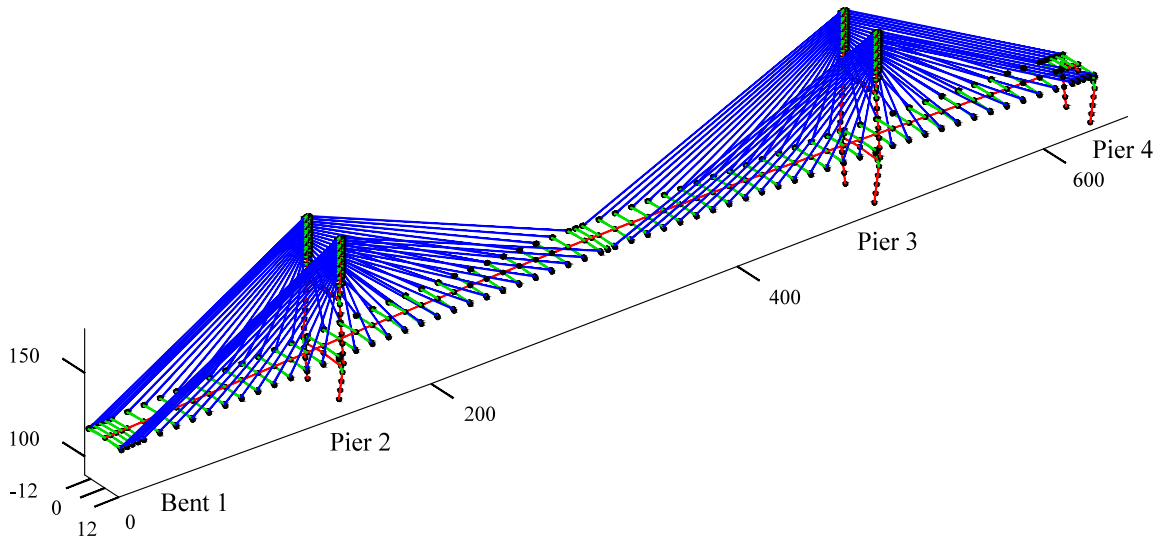

Figure 1: Finite element model of the bridge (dimensions in m); adapted from Dyke et al. (2003).

where $\mathbf{M}_s$, $\mathbf{C}_s$, and $\mathbf{K}_s$ are the mass, damping and stiffness matrices, respectively, of the bridge superstructure for the active DOFs; $\mathbf{r}$ is the influence vector for the ground acceleration (containing ones in entries corresponding to active displacements in the direction of the 1-D horizontal excitation and zeros elsewhere); $\mathbf{u}_s(t)$ is the generalized displacement vector; and $\ddot{u}_g(t)$ is the ground acceleration in the longitudinal direction. The reader is directed to the benchmark definition paper (Dyke et al., 2003) for further details of this model.

3.2. Passive damping devices

Two types of passive devices are investigated: q_u nonlinear viscous dampers and q_d nonlinear tuned mass dampers (TMDs). The damping forces in the viscous dampers follow the power-law relation

$$f_i^u = c_i^u |\Delta\dot{u}_i|^{\beta_i^u} \operatorname{sgn}(\Delta\dot{u}_i), \quad i = 1,\ldots,q_u \tag{11}$$

where $\Delta\dot{u}_i$ is the velocity across the i^{th} damper. The governing differential equations of the TMD mass motions are given by,

$$\begin{aligned} m_i^d\ddot{v}_i + c_i^d|\dot{\Delta v}_i|^{\beta_i^d}\operatorname{sgn}(\dot{\Delta v}_i) + k_i^d\Delta v_i \\ = -m_i^d r_i^d \ddot{u}_g, \quad i = 1,\ldots,q_d \end{aligned} \tag{12}$$

where v_i is the displacement of the TMD relative to the ground, Δv_i is the TMD displacement relative to its attachment point on the bridge, and r_i^d is in $[-1,1]$ depending on the TMD's orientation relative to the earthquake ground motion direction.

To be consistent with the symmetric nature of the bridge model, the passive devices are placed in identical pairs symmetrically located about the bridge deck centerline; *i.e.*, let $c_{2i-1}^u = c_{2i}^u$ and $\beta_{2i-1}^u = \beta_{2i}^u$ for $i = 1,\ldots,q_u$ (dampers) and $c_{2i-1}^d = c_{2i}^d$, $\beta_{2i-1}^d = \beta_{2i}^d$, $m_{2i-1}^d = m_{2i}^d$ and $r_{2i-1}^d = r_{2i}^d$ for $i = 1,\ldots,q_d$ (TMDs). Further, this example considers each pair of nonlinear viscous dampers as uncertain — $\boldsymbol{\delta} = \left[c_2^u \quad \beta_2^u \mid c_4^u \quad \beta_4^u \mid \ldots \mid c_{q_u}^u \quad \beta_{q_u}^u\right]^T$ — and the stiffness and damping of each pair of TMDs as the design parameters — $\boldsymbol{\theta} = \left[c_2^d \quad \beta_2^d \quad k_2^d \mid c_4^d \quad \beta_4^d \quad k_4^d \mid \ldots \mid c_{q_d}^d \quad \beta_{q_d}^d \quad k_{q_d}^d\right]^T$. The ratio of TMD masses relative to bridge mass is fixed at a certain value.

3.3. Formulation

The bridge equations of motion can be written in form of (1) where,

$$\mathbf{X}(t) = \begin{Bmatrix} \mathbf{u}(t) \\ \dot{\mathbf{u}}(t) \end{Bmatrix}, \mathbf{A} = \begin{bmatrix} \mathbf{0} & \mathbf{I} \\ -\mathbf{M}^{-1}\mathbf{K} & -\mathbf{M}^{-1}\mathbf{C} \end{bmatrix},$$

$$\mathbf{B} = \begin{Bmatrix} \mathbf{0} \\ \bar{\mathbf{r}} \end{Bmatrix}, \mathbf{L}_u = \begin{bmatrix} \mathbf{0} \\ -\mathbf{M}^{-1}\mathbf{R}_u \end{bmatrix}, \mathbf{L}_d = \begin{bmatrix} \mathbf{0} \\ -\mathbf{M}^{-1}\mathbf{R}_d \end{bmatrix},$$

$$\mathbf{u}(t) = \begin{Bmatrix} \mathbf{u}_s(t) \\ \mathbf{v}(t) \end{Bmatrix}, \mathbf{M} = \begin{bmatrix} \mathbf{M}_s & \mathbf{0} \\ \mathbf{0} & \mathbf{M}_d \end{bmatrix}, \mathbf{K} = \begin{bmatrix} \mathbf{K}_s & \mathbf{0} \\ \mathbf{0} & \mathbf{0} \end{bmatrix},$$

and $\mathbf{C} = \begin{bmatrix} \mathbf{C}_s & \mathbf{0} \\ \mathbf{0} & \mathbf{0} \end{bmatrix}$; $\mathbf{M}_d$ is a diagonal matrix of TMD masses; $\bar{\mathbf{r}} = [\mathbf{r}^T \quad r_1 \ldots r_{q_d}]^T$ is the influence

vector for the ground acceleration; $\mathbf{R}_\mathrm{u}$ and $\mathbf{R}_\mathrm{d}$ are the influence matrices for the uncertain damper forces and the TMD forces (from design parameters), respectively. Each of the q_u columns of $\mathbf{R}_\mathrm{u}$ and q_d columns of $\mathbf{R}_\mathrm{d}$ transform the pseudoforce of one passive device to a global force vector, with

$$\mathbf{g}_\mathrm{u}(\overline{\mathbf{X}}_\mathrm{u}(t);\boldsymbol{\delta}) = \begin{bmatrix} -c_2^\mathrm{u}|\Delta\dot{u}_1|^{\beta_2^\mathrm{u}}\,\mathrm{sgn}(\Delta\dot{u}_1) \\ -c_2^\mathrm{u}|\Delta\dot{u}_2|^{\beta_2^\mathrm{u}}\,\mathrm{sgn}(\Delta\dot{u}_2) \\ \hline \vdots \\ \hline -c_{q_\mathrm{u}}^\mathrm{u}|\Delta\dot{u}_{q_\mathrm{u}-1}|^{\beta_{q_\mathrm{u}}^\mathrm{u}}\,\mathrm{sgn}(\Delta\dot{u}_{q_\mathrm{u}-1}) \\ -c_{q_\mathrm{u}}^\mathrm{u}|\Delta\dot{u}_{q_\mathrm{u}}|^{\beta_{q_\mathrm{u}}^\mathrm{u}}\,\mathrm{sgn}(\Delta\dot{u}_{q_\mathrm{u}}) \end{bmatrix},$$

where $\overline{\mathbf{X}}_\mathrm{u}(t) = \begin{bmatrix}\Delta\dot{u}_1 & \Delta\dot{u}_2 \mid \ldots \mid \Delta\dot{u}_{q_\mathrm{u}-1} & \Delta\dot{u}_{q_\mathrm{u}}\end{bmatrix}^\mathrm{T} = \mathbf{G}_\mathrm{u}\mathbf{X}(t) = \begin{bmatrix}\mathbf{0} & \mathbf{R}_\mathrm{u}^\mathrm{T}\end{bmatrix}\mathbf{X}(t)$ and

$$\mathbf{g}_\mathrm{d}(\overline{\mathbf{X}}_\mathrm{d}(t);\boldsymbol{\theta}) = \begin{bmatrix} -c_2^\mathrm{d}|\Delta\dot{v}_1|^{\beta_2^\mathrm{d}}\,\mathrm{sgn}(\Delta\dot{v}_1) \\ -k_1^\mathrm{d}\Delta\dot{v}_1 \\ -c_2^\mathrm{d}|\Delta\dot{v}_2|^{\beta_2^\mathrm{d}}\,\mathrm{sgn}(\Delta\dot{v}_2) \\ -k_2^\mathrm{d}\Delta\dot{v}_2 \\ \hline \vdots \\ \hline -c_{q_\mathrm{d}}^\mathrm{d}|\Delta\dot{v}_{q_\mathrm{d}-1}|^{\beta_{q_\mathrm{d}}^\mathrm{d}}\,\mathrm{sgn}(\Delta\dot{v}_{q_\mathrm{d}-1}) \\ -k_{q_\mathrm{d}}^\mathrm{d}\Delta\dot{v}_{q_\mathrm{d}-1} \\ -c_{q_\mathrm{d}}^\mathrm{d}|\Delta\dot{v}_{q_\mathrm{d}}|^{\beta_{q_\mathrm{d}}^\mathrm{d}}\,\mathrm{sgn}(\Delta\dot{v}_{q_\mathrm{d}}) \\ -k_{q_\mathrm{d}}^\mathrm{d}\Delta\dot{v}_{q_\mathrm{d}} \end{bmatrix}$$

where $\overline{\mathbf{X}}_\mathrm{d}(t) = [\Delta v_1 \quad \Delta\dot{v}_1 \quad \Delta v_2 \quad \Delta\dot{v}_2 \mid \ldots \mid \Delta v_{q_\mathrm{d}-1} \quad \Delta\dot{v}_{q_\mathrm{d}-1} \quad \Delta v_{q_\mathrm{d}} \quad \Delta\dot{v}_{q_\mathrm{d}}]^\mathrm{T} = \mathbf{G}_\mathrm{d}\mathbf{X}(t) = [\mathbf{0} \quad \mathbf{R}_\mathrm{d}^\mathrm{T}]\mathbf{X}(t)$.

3.4. Objective function and constraints

The goal of this example is to optimize the parameters of the TMDs to improve the bridge's performance given uncertainties in the nonlinear viscous dampers installed elsewhere in the bridge. Different performance metrics can be chosen; a set of metrics, normalized with respect to the uncontrolled and connected deck-tower case suggested by Dyke et al. (2003), are used here subject to the 1940 El Centro earthquake excitation. As in Dyke et al. (2003): $F_{bi}(t)$ and $M_{bi}(t)$ are the base shear and overturning moment, respectively, at the i^th tower at time t; $F_{di}(t)$ and $M_{di}(t)$ are the corresponding deck-level shear and overturning moment; $||\cdot(t)||$ denotes the root mean square (*i.e.*, two-norm over time) response; $(\cdot)_{0(\cdot)}^\mathrm{max}$ denotes the maximum, over both time and tower number, uncontrolled base or deck-level shear or overturning moment at the base or deck level; and $||(\cdot)_{0(\cdot)}(t)||$ denotes the maximum, over tower number, time-normed uncontrollable shear or overturning moment at the base or deck level. Then, eight of the metrics used to form the objective function and some constraints are,

$$\begin{aligned} J_1 &= \frac{\max_{i,t}|F_{bi}(t)|}{F_{0b}^\mathrm{max}}, \quad J_2 = \frac{\max_{i,t}|F_{di}(t)|}{F_{0d}^\mathrm{max}}, \\ J_7 &= \frac{\max_{i}||F_{bi}(t)||}{||F_{0b}(t)||}, \quad J_8 = \frac{\max_{i}||F_{di}(t)||}{||F_{0d}(t)||} \\ J_3 &= \frac{\max_{i}|M_{bi}(t)|}{M_{0b}^\mathrm{max}}, \quad J_4 = \frac{\max_{i}|M_{di}(t)|}{M_{0d}^\mathrm{max}}, \\ J_9 &= \frac{\max_{i,t}||M_{bi}(t)||}{||M_{0b}(t)||}, \quad J_{10} = \frac{\max_{i,t}||M_{di}(t)||}{||M_{0d}(t)||} \end{aligned} \tag{13}$$

Additional metrics used in the constraints are

$$J_6 = \max_{i,t}\left|\frac{x_{bi}(t)}{x_{0b}}\right|, \quad J_{12} = \max_{i,t}\frac{f_i(t)}{W}, \tag{14}$$

where $x_{bi}(t)$ is the displacement of the deck at the two ends (Bent 1 and Pier 4) in the finite element model at time t; x_{0b} is the maximum, over time and end locations, of the uncontrolled displacement of the deck; $f_i(t)$ is the amount of force exerted by the i^th device, assumed here to be the TMD; and $W = 510$ MN is the weight of the bridge superstructure. The normed responses are calculated using 200 s of response as suggested by Dyke et al. (2003). (Note: performance metrics J_5, J_{11} and J_{13} through J_{18}, defined in the benchmark (Dyke et al., 2003), are not used herein.)

Using these performance metrics, the deterministic optimization problem is formulated as

$$\begin{aligned} &\min_{\boldsymbol{\theta}\in\boldsymbol{\Theta}} J_1(\boldsymbol{\theta}) \\ &\text{subject to} \quad J_k(\boldsymbol{\theta}) \le \alpha J_{k,0} \quad \forall k \in \{2\text{–}4, 7\text{–}10\} \end{aligned} \tag{15}$$

where $\boldsymbol{\Theta} = \{\boldsymbol{\theta} : k^\mathrm{lb} \le \theta_{3j-2} \le k^\mathrm{ub}, c^\mathrm{lb} \le \theta_{3j-1} \le c^\mathrm{ub}, \beta^\mathrm{lb} \le \theta_{3j} \le \beta^\mathrm{ub}, \ j = 1,\ldots,q_\mathrm{d}\}$; $J_{k,0}$ corresponds to the k^th performance metric without dampers (i.e. $c_i^\mathrm{d} = 0$, $k_i^\mathrm{d} = 0$); $(\cdot)^\mathrm{lb}$ and $(\cdot)^\mathrm{ub}$ are lower and upper bounds on the design parameters; and α is set to 1.25 (De et al., 2015). Each TMD is designed with a mass that is 2% of the bridge mass; *i.e.*, $m_i^\mathrm{d} = 0.02W/g$ for $i = 1,\ldots,q_\mathrm{d}$.

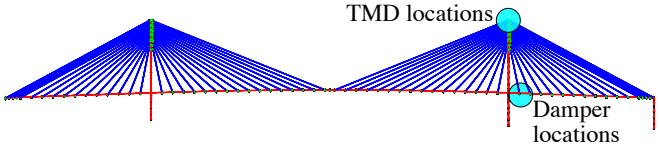

Figure 2: Finite element model (side view) of the bridge; adapted from Dyke et al. (2003).

For simplicity, consider the case of a single pair of TMDs attached on top of the 2nd tower as shown in Figure 2. The initial values k_0 and c_0 of the design parameters for the optimization problem are taken from the guidelines specified in Hoang et al. (2008) for the first mode of vibration with $\beta_0 = 1.0$ (clearly, any optimization should evaluate the effect of different initial values; here, with different initial design points, the objective function minimum was found to be relatively insensitive though the optimum design point may change). The lower and upper bounds for stiffness and damping coefficients are taken as [50 kN/m, 5 MN/m] and [100 kN·(s/m)$^{\beta}$, 6 MN·(s/m)$^{\beta}$], respectively, after preliminary studies indicated that the optimum parameters are expected to lie in these ranges. The lower and upper limits for β are taken as 0.2 and 1.8 as suggested by Main and Jones (2002).

This optimization problem is then modified to include the design under uncertainty formulation. The uncertain parameter vector corresponds to a single pair of nonlinear dampers (*i.e.*, $q_{\mathrm{u}} = 2$), one placed connecting nodes 319 and 186 in the finite element model and the other symmetrically connecting nodes 324 and 119 (see Figure 2). The uncertain parameters of the passive dampers follow the distributions given in Table 1, where the mean values were obtained from a deterministic optimization similar to (15) performed over a set of possible passive viscous damper locations and parameters with $c \in [0.5, 30]$ MN·(s/m)$^{\beta}$ and $\beta \in [0.2, 1.8]$.

Table 1: Uncertain parameter description

Variable	Distribution	Mean	COV
Damping coeff.(c_2^{u})	Log-normal	20.5440 MN·(s/m)$^{\beta_2^{\mathrm{u}}}$	0.05
Exponent (β_2^{u})	Log-normal	0.9777	0.1

Note: COV = coefficient of variation

3.5. Optimization Results

The optimization is performed using MATLAB's `fmincon` with default values for tolerances but limited to 50 function evaluations (actual results may slightly exceed 50 since each iteration may perform multiple function evaluations). An active-set algorithm (*sequential quadratic programming*) is used inside `fmincon`. While `fmincon` can be provided with gradient information, a finite difference approximation is used here to evaluate the gradients.

A preliminary study of this problem showed that $N_{\boldsymbol{\delta}} = 100$ samples, using Latin Hypercube sampling method with antithetic variates variance reduction (Ayyub and Lai, 1991), were sufficient to give converged results for the average design optimization (though the number of samples clearly depends on the application and the optimization objective and constraints). The results of the design optimization are shown in Tables 2 and 3. The optimal values for k_2^{d} are similar for both average and worst case design; however the optimal values for

Table 2: Worst-case design of nonlinear TMD

Reduction of cost: max J_1 (in %)		# fcn. evals.
26.4922		51
k_2^{d} [MN/m]	c_2^{d} [MN · (s/m)$^{\beta_2^{\mathrm{d}}}$]	β_2^{d}
0.9086	3.8165	0.2000

Table 3: Average design of nonlinear TMD

Reduction of cost: $\mathbb{E}[J_1]$ (in %)		# fcn. evals.
7.3690		53
k_2^{d} [MN/m]	c_2^{d} [MN · (s/m)$^{\beta_2^{\mathrm{d}}}$]	β_2^{d}
0.8453	1.9186	1.0826

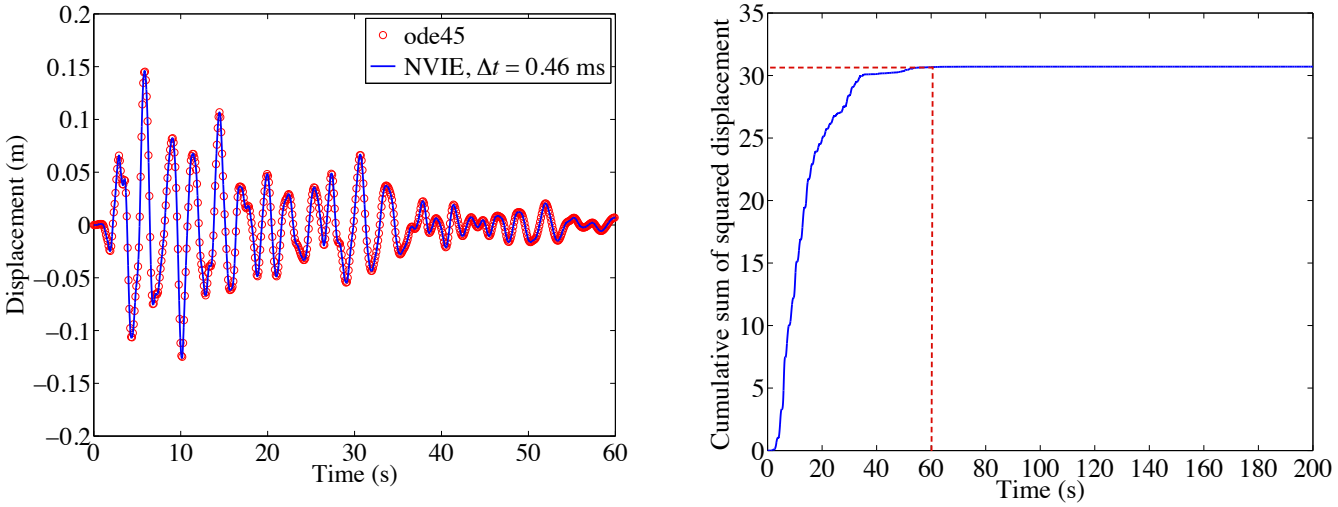

(a) Accuracy in a typical generalized displacement *(b) Cumulative sum of a typical squared response*

Figure 3: Accuracy of the NVIE approach for first 60 s compared to MATLAB*'s* `ode45`

c_2^{d} and β_2^{d} differ significantly. In the worst case design, the value of device force performance metric J_{12} increases to 3.19 times that of the average design case. A deterministic optimization for the TMD parameters with mean values for the passive dampers gives $k_{\mathrm{opt}} = 0.9503$ MN/m, $c_{\mathrm{opt}} = 0.3896$ MN·(s/m)$^{\beta_{\mathrm{opt}}}$, $\beta_{\mathrm{opt}} = 0.7568$, which gives a lower peak device force and 0.29 times J_{12} than average design case. Hence, due to the assumed uncertainty in the structure, the robust optimization requires a TMD capable of exerting greater force.

3.6. Computational Efficiency

The nonlinear Volterra integral equation approach involves a one-time cost and repeated costs for each iteration of the design under uncertainty framework. The one-time computational cost involves solution of $\mathbf{x}(t)$ in (3) and calculation of $\mathbf{H}_{\mathrm{L}}$. The repeated cost involves solution of (5) and for the resulting outputs $\mathbf{Y}(t)$ for different uncertainty and design parameters. To evaluate the computational cost of the proposed method, it is compared with a fixed time step 4$^{\mathrm{th}}$ order Runge-Kutta method (RK-4). The RK-4 method diverges for $\Delta t = 1$ ms or higher because of the numerical stiffness of the system of differential equations of motion. Hence, $\Delta t = 0.5$ ms is used for RK-4, giving a relative accuracy of $\mathcal{O}(10^{-3})$ computed relative to the `ode45` with relative tolerance of 10^{-6} and absolute tolerance of 10^{-8} (for just the first 60 s of response which provides RMS close to the long term as shown in Figure 3b; only 60 s is used because the full `ode45` solution takes too much time). The proposed NVIE approach gives relative accuracy in RMS of states in the same order with $\Delta t = 0.46$ ms.

For $N_{\boldsymbol{\delta}} = 100$, and for 10 function evaluations in the optimization procedure, $\mathbf{x}^{(\mathrm{nl})}(t)$ must be evaluated a total of 1000 times. Computation times are evaluated using MATLAB's `cputime` function on a computer with a 2.3 GHz Core i7-4850HQ processor, 16 GB RAM, Mac OS X, and running MATLAB 2013a. The proposed NVIE approach takes 13.53 cpu-min. to compute $\mathbf{p}(t)$, 2.16 cpu-min. to compute $\mathbf{Y}(t)$ in each repeated calculation and a total 10.92 cpu-days for 1000 simulations. However RK-4 requires the full solution a total 1000 times, where each simulation takes 77.66 cpu-hrs., which projects to a total of 8.87 cpu-years for the full optimization. Hence, the proposed design-under-uncertainty framework provides a computational speedup of 296.33 with comparable accuracy. While only 3 design variables are considered here, comparable or increased gains in computational efficiency, relative to other approaches for simulating the system responses for the function evaluations, are expected when more design variables are used.

4. CONCLUSIONS

Structural design under uncertainties provides many computational challenges. The proposed

method shows significant computational advantages for such problems. In future work, the reliability based design optimization will be incorporated in this framework; further, design optimization under uncertainty of structural systems, with passive control devices, subjected to random excitation will be considered in subsequent studies.

ACKNOWLEDGMENTS

The authors gratefully acknowledge the partial support of this work by the National Science Foundation through awards CMMI 13-44937 and 14-36018. Any opinions, findings, and conclusions or recommendations expressed in this material are those of the authors and do not necessarily reflect the views of the National Science Foundation. The authors also acknowledge the support of the first author by the Provost's Ph.D. Fellowship at the University of Southern California.

5. REFERENCES

Adeli, H. (2002). *Advances in design optimization*. CRC Press.

Ayyub, B. M. and Lai, K.-L. (1991). "Selective sampling in simulation-based reliability assessment." *International Journal of Pressure Vessels and Piping*, 46(2), 229–249.

Beck, J., Papadimitriou, C., Chan, E., and Irfanoglu, A. (1996). "Reliability-based optimal design decisions in the presence of seismic risk." *Proceedings 11th World Conference on Earthquake Engineering*, Pergamon.

Beck, J. L., Chan, E., Irfanoglu, A., and Papadimitriou, C. (1999). "Multi-criteria optimal structural design under uncertainty." *Earthquake Engineering and Structural Dynamics*, 28(7), 741–762.

Calafiore, G. C. and Dabbene, F. (2008). "Optimization under uncertainty with applications to design of truss structures." *Structural and Multidisciplinary Optimization*, 35(3), 189–200.

De, S., Wojtkiewicz, S. F., and Johnson, E. A. (2015). "Computationally efficient optimal design of passive control devices for a benchmark cable-stayed bridge." *Structural Control and Health Monitoring*, in preparation.

Dyke, S. J., Caicedo, J. M., Turan, G., Bergman, L., and Hague, S. (2003). "Phase I benchmark control problem for seismic response of cable-stayed bridges." *Journal of Structural Engineering*, 129(7), 857–872.

Enevoldsen, I. and Sørensen, J. D. (1994). "Reliability-based optimization in structural engineering." *Structural Safety*, 15(3), 169–196.

Frangopol, D. M. (1985). "Multicriteria reliability-based structural optimization." *Structural Safety*, 3(1), 23–28.

Gasser, M. and Schuëller, G. I. (1997). "Reliability-based optimization of structural systems." *Mathematical Methods of Operations Research*, 46(3), 287–307.

Gaurav, Wojtkiewicz, S. F., and Johnson, E. A. (2011). "Efficient uncertainty quantification of dynamical systems with local nonlinearities and uncertainties." *Prob. Eng. Mech.*, 26(4), 561–569.

Hoang, N., Fujino, Y., and Warnitchai, P. (2008). "Optimal tuned mass damper for seismic applications and practical design formulas." *Engineering Structures*, 30(3), 707–715.

Kamalzare, M., Johnson, E. A., and Wojtkiewicz, S. F. (2015). "Efficient optimal design of passive structural control applied to isolator design." *Smart Structures and Systems*, in press.

Linz, P. (1985). *Analytical and numerical methods for Volterra equations*, Vol. 7. SIAM.

Main, J. and Jones, N. (2002). "Free vibrations of taut cable with attached damper. II: Nonlinear damper." *Journal of Engineering Mechanics*, 128(10), 1072–1081.

Papadrakakis, M. and Lagaros, N. D. (2002). "Reliability-based structural optimization using neural networks and Monte Carlo simulation." *Computer Methods in Applied Mechanics and Engineering*, 191(32), 3491–3507.

Sandgren, E. and Cameron, T. (2002). "Robust design optimization of structures through consideration of variation." *Computers & Structures*, 80(20), 1605–1613.

Tu, J., Choi, K. K., and Park, Y. H. (1999). "A new study on reliability-based design optimization." *Journal of Mechanical Design*, 121(4), 557–564.

Zang, C., Friswell, M., and Mottershead, J. (2005). "A review of robust optimal design and its application in dynamics." *Computers & Structures*, 83(4), 315–326.